

Origin of Colossal Dielectric Response of $\text{Pr}_{0.6}\text{Ca}_{0.4}\text{MnO}_3$

N. Biškup,* A. de Andrés, and J.L. Martínez

Instituto de Ciencia de Materiales, CSIC, Cantoblanco 28049 Madrid, Spain

C. Perca

Laboratoire de Physico-Chimie de l'Etat Solide, Université Paris XI, 91405 Orsay Cedex - France

(Dated: February 2, 2008)

We report the detailed study of dielectric response of $\text{Pr}_{0.6}\text{Ca}_{0.4}\text{MnO}_3$ (PCMO), member of manganite family showing colossal magnetoresistance. Measurements have been performed on four polycrystalline samples and four single crystals, allowing us to compare and extract the essence of dielectric response in the material. High frequency dielectric function is found to be $\epsilon_0=30$, as expected for the perovskite material. Dielectric relaxation is found in frequency window of 20Hz-1MHz at temperatures of 50-200K that yields to colossal low-frequency dielectric function, i.e. static dielectric constant. Static dielectric constant is always colossal, but varies considerably in different samples from $\epsilon_0=10^3$ until 10^5 . The measured data can be simulated very well by blocking (surface barrier) capacitance in series with sample resistance. This indicates that the large dielectric constant in PCMO arises from the Schottky barriers at electrical contacts. Measurements in magnetic field and with d.c. bias support this interpretation. Colossal magnetocapacitance observed in the title compound is thus attributed to extrinsic effects. Weak anomaly at the charge ordering temperature can also be attributed to interplay of sample and contact resistance. We comment our results in the framework of related studies by other groups.

PACS numbers: 77.22.Ch, 75.47.Lx, 75.47.Gk

Introduction

The typical value of dielectric constant $\epsilon(0)$ in solids is of the order 1-10. Exceptions are ferroelectrics with $\epsilon(0)\approx 10^4$ and (charge/spin) density waves materials (CDW/SDW) with $\epsilon(0)\approx 10^7\text{-}10^9$. In the former the large dielectric response is a consequence of charge polarization due to ferroelectric displacement of central ion in the unit cell. In the latter, large polarization is achieved by local displacement of electron condensate in density wave. But both of them are unsuitable for applications: ferroelectrics due to limited temperature and frequency range around ferroelectric transition and CDW/SDW materials due to inapplicably low temperatures where density waves occur.

It is therefore understandable that discovery of room temperature frequency independent "colossal" dielectric constant of complex perovskite compound $\text{CaCu}_3\text{Ti}_4\text{O}_{12}$ (CCTO)¹ sparked the interest in new materials that might not be limited by frequency and temperature. At room temperature CCTO has high dielectric constant ($\epsilon(0)\approx 10^4\text{-}10^5$) that was confirmed in ceramic samples, single crystals and thin films. Theoretical modeling has excluded the possibility of intrinsic origin of high $\epsilon(0)$ ². These studies conclude that the internal inhomogeneities are in the origin of the effect. It is suspected that those inhomogeneities arise from crystal twinning or some internal domain boundaries. On the other hand, some authors interpret high dielectric response as an artifact coming from Schottky effect at the electrode contacts³. In order to solve this dispute, it is useful to study dielectric response in other materials that are known to be inhomogeneous. Manganites are excellent candidates for this purpose.

The family of manganites has attracted a widespread attention of scientific community in the last 15 years due to their "colossal" magnetoresistance⁴. The magnetoresistive effects in some compositions reach the factor of 10^6 , which essentially means magnetic field induced insulator-metal transitions. In order to understand such colossal effects, the concept of phase separation has emerged. The ground state of certain manganite compounds^{5,6} is proved to be inhomogeneous, consisting typically of metallic clusters in an insulating/semiconducting matrix. Such a separation of phases (metallic and insulating) is believed to be the cause of many unusual phenomena, including colossal magnetoresistance. The purpose of this work is to investigate if the phase separating boundaries can contribute to the dielectric response.

The general formula for manganites is $\text{R}_{1-x}\text{A}_x\text{MnO}_3$ where R stands for rare earth (La, Pr) and A for any divalent atom (Ca, Sr). Among various manganites, $\text{Pr}_{1-x}\text{Ca}_x\text{MnO}_3$ is unique, showing insulating behaviour over the whole composition (x) range due to its narrow bandwidth of 3d conducting e_g electrons⁷. The title compound $\text{Pr}_{0.6}\text{Ca}_{0.4}\text{MnO}_3$ falls in the range $0.3 < x < 0.75$ where the ground state is charge ordered antiferromagnetic insulator^{8,9}. Charge ordering refers to ordering of manganese ions that can be in Mn^{3+} or Mn^{4+} valence: at low temperatures these ions order into a superstructure forming stripes of Mn^{3+} and Mn^{4+} ions. Magnetization measurements in the title compound show two transitions at $T=240$ and $T=180\text{K}$ that are believed to be charge (T_{CO}) and antiferromagnetic ordering (T_{AF}), respectively. Insulator-metal transition in title compound can be induced by magnetic field⁷, electric current¹⁰,

pressure¹¹ or X-rays¹². These and other studies^{13,14,15} converged around the idea of phase separation involving ferromagnetic metallic droplets coalescing and enabling the current percolation through the insulating matrix. The origin of phase separation lies in existence of structural inhomogeneities (clusters) associated with charge ordering^{16,17}. Recent report of nanoscale competition in charge ordered LCMO¹⁸ concludes that even the same phases (charge ordered insulator) form clusters with different orientation of CO stripes. The formation of clusters generally precedes structural or magnetic transitions¹⁹ arising at temperature $T^* > T_C$ (in our case $T_C = T_{CO}$). PCMO system is thus ideal to study dielectric response of the inhomogeneous (clustered) system. Initial reports of giant dielectric response in $\text{Pr}_{0.67}\text{Ca}_{0.33}\text{MnO}_3$ ($x=1/3$) appeared in year 1999²⁰ and the most recent one in 2004²¹. In the latter case it is suggested that it arises from CDW orderings or phase separation inhomogeneities. We have performed detailed study on similar system (PCMO with $x=3/8$) in order to resolve the origin of apparent colossal dielectric response in PCMO.

After this introduction, we give an overview of experimental methods. In results we report on four topics: resistive characterization, dielectric response in temperature, influence of magnetic field and influence of d.c. bias. Discussion is following each of these measurement reports. In Summary we bring the conclusions and comment our findings in the light of related reports.

Experimental

We have measured 4 polycrystalline (PC) samples (P1-P4) and 4 single crystals (SC, S1-S4) which enables us to extract the data inherent to the material itself and test and compare the findings. Single crystal samples are plates that are cut from the single rod. A Laue pattern taken on the growth direction of the single crystal indicated the coincidence with the [001] direction, inside 15 degree, or even less. Single crystal measurements for samples S1-S3 are with current contacts in this [001] direction while contacts for S4 are in perpendicular direction. The nominal composition of polycrystals ($\text{Pr}_{0.6}\text{Ca}_{0.4}\text{MnO}_3$) differs slightly from the single crystals ($\text{Pr}_{0.625}\text{Ca}_{0.375}\text{MnO}_3$) but their characterization shows almost identical behaviour (Figure 1). Samples are first characterized magnetically (SQUID), later electrically (four-contact configuration) and then prepared for the capacitance measurements (two-contact configuration). Care was taken to reduce the parasite capacitances of measurement system below 3pF in order to have measurable signal even in the high frequency limit (ε_{HF}). Dielectric measurements are done with Quadtech LCR-meter, model 1920. The voltage applied was always at low limit of 20mV in order to minimize the effects of voltage-current nonlinearity. The frequency range covered by this instrument lies between 20Hz and 1MHz. At low temperatures the relaxation times for colossal dielectric response drop below our frequency window. Here we measured dielectric constant/capacitance through the

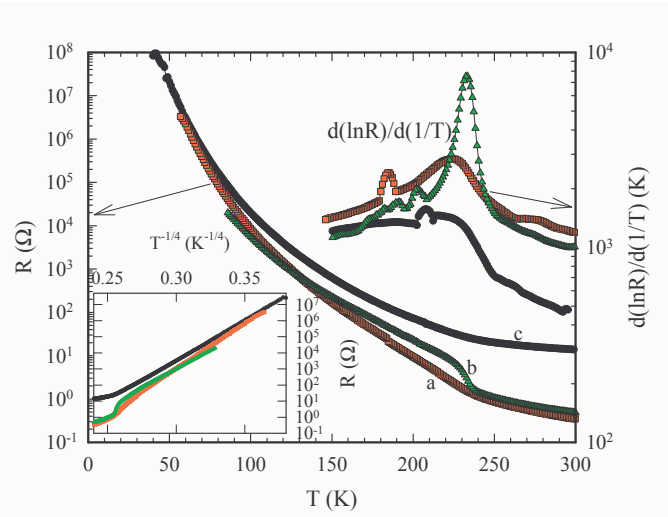


FIG. 1: (Color online) Temperature dependent resistance of polycrystal P1 $\text{Pr}_{0.6}\text{Ca}_{0.4}\text{MnO}_3$ (a, squares) and single crystal S1 $\text{Pr}_{5/8}\text{Ca}_{3/8}\text{MnO}_3$ (b, triangles). Circles (c) stand for two contact (capacitance) configuration of P1 sample. In the right inset is $d(\ln R)/d(1/T)$ indicating T_{CO} . In the left inset is resistance over $T^{-1/4}$ indicating three dimensional variable range hopping.

time dependent charging effect by sourcemeter Keithley 2410.

Results and discussion

Resistive characterization

Figure 1 shows the resistive characterization of representative polycrystalline (P1) and single crystal (S1) samples. The charge ordering transition, interpreted as the peak in the derivative $d(\ln R)/d(1/T)$, appears at $T_{CO}=225$ and 235K , respectively. These values are very close, especially in the light of "broad" peak in polycrystalline sample. Magnetization data give identical value for both cases of $T_{CO}=235\text{K}$. The antiferromagnetic ordering at 175 K is detectable only in the magnetization measurements. Small peaks in derivative curves at $T \leq 200\text{K}$ are consequence of single-point cracks in resistivity measurements and therefore not related to antiferromagnetic ordering. The insulating behavior below T_{CO} is governed by three-dimensional ($d=3$) variable range hopping²² where electrical conductivity follows

$$\sigma_{DC} = \sigma_0 e^{-(\frac{T_0}{T})^{\frac{1}{1+d}}} \quad (1)$$

Further, all data from resistive measurements (resistivity in polycrystal and two perpendicular directions in single crystals, as well as measurements in magnetic field) show no sign of anisotropy. This enables us to treat identically the dielectric response in polycrystalline and single crystal samples. From Figure 1 we can also estimate the influence of contact resistances in two-probe measurements, which, as expected, becomes negligible at low

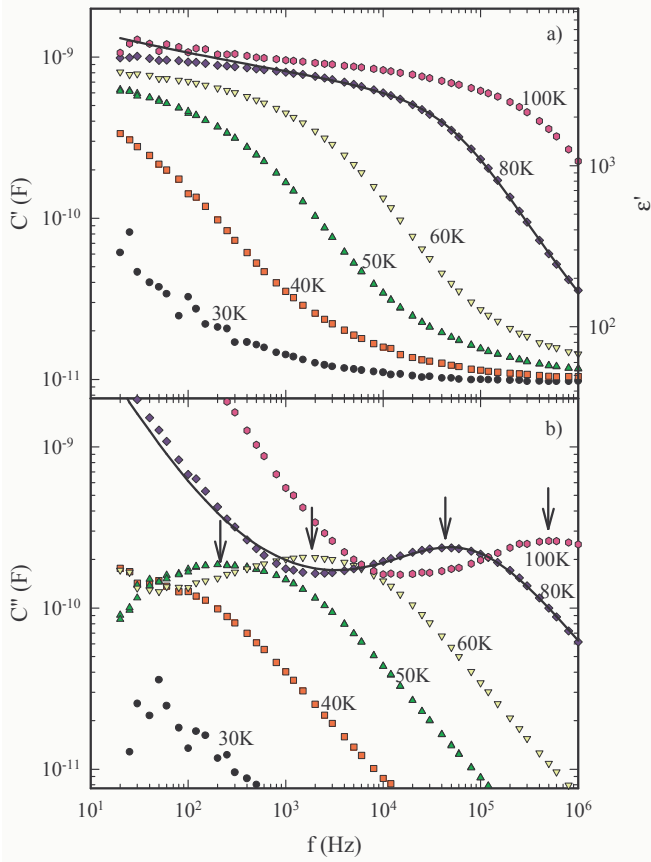


FIG. 2: (Color online) Dielectric relaxation for polycrystal P1 at temperatures given in the figures. a) $C'(\omega)$. On the right scale is value of dielectric function. b) $C''(\omega)$. Arrows denote loss peaks. Line is the fit to 80K data as defined in text.

temperatures.

Dielectric response and its temperature dependence

The most instructive presentation of dielectric data is given in the terms of frequency dependent dielectric permittivity/capacitance²³ - the method that is followed here. Dielectric data are collected measuring real (G) and imaginary (B) part of electrical admittance. Capacitance is directly related to dielectric constant as $C = \epsilon_0 \epsilon(s/l)$ and in this report we present data in this form. Figures 2 shows the typical frequency response of PCMO system: Fig 2a shows real and Fig 2b imaginary part of complex capacitance $C^* = C' + iC''$. The data in figures 2 correspond to P1 polycrystal but represent very well the response of all eight samples. The low-frequency relaxation shown in Fig. 2 is very reminiscent to Debye relaxation, having well defined 'loss peak' in ϵ'' . Phenomenologically, such relaxation is given by:

$$\epsilon(\omega) = \epsilon_{HF} + [\epsilon(0) - \epsilon_{HF}] \frac{1}{1 - i\omega\tau_0} \quad (2)$$

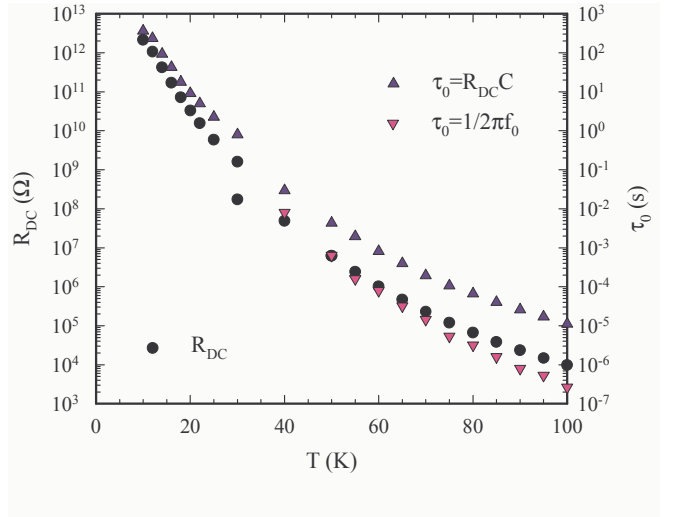


FIG. 3: (Color online) Fig. 3 Relaxation time τ_0 as a function of temperature (triangles - right axis). See text for point assignment. On the left axis is samples resistance (solid circles).

where τ_0 denotes characteristic low-frequency relaxation time $\tau_0 = 1/\omega_0$. $\epsilon(0)$ is dielectric constant and ϵ_{HF} stands for high frequency dielectric function, i.e. at $\omega \gg \omega_0 = 1/\tau_0$. In the limit $\epsilon_{HF} \rightarrow 0$ this expression corresponds to 'Debye' equivalent circuit consisting of resistance R coupled serially to capacitance C. Relaxation time τ_0 in such equivalent circuit is given by $\tau_0 = RC$ and at frequencies above relaxation ($\omega > \omega_0 = 1/\tau_0$, real and imaginary part of complex 'capacitance' follow ω^{-2} and ω^{-1} dependence, respectively. Note however that corresponding exponents in Fig. 2 are lower than in this ideal (Debye) case. This is usually interpreted in the terms of distribution of relaxation times.

Figure 3 shows the resistance R of sample P1 (left axis) plotted together with 'Debye' relaxation time $\tau_0 = 1/\omega_0$ (right axis) for temperatures below 100K. All data are from two contact capacitance measurements. Solid circles denote R_{DC} data taken by LCR-meter. At $T \leq 30K$ relaxation falls below our frequency window. At these temperatures capacitance C and resistance R are measured through time dependence of charging process. Voltage at the electrodes is built up according to $V(t) = V_0(1 - e^{-t/\tau_C})$, which extends our temperature range for capacitance measurements down to $T = 10K$. Triangles pointing up are simply product of resistance and capacitance $\tau_0 = R_{DC}C$, while those pointing down are taken from the loss peak frequency $\tau_0 = 1/(2\pi f_0)$, as indicated in figure 2b. One can see that τ_0 follows fairly well the temperature behavior of resistance. This shouldn't be surprising if dielectric screening arises from the same carriers that contribute to electric conductivity. The discrepancy of two "definitions" of τ_0 decreases with decreasing temperature and tends to diminish at very low temperatures where contact resistance becomes negligible comparing to intrinsic sample resistance entering into $\tau_0 = R_{DC}C$. This

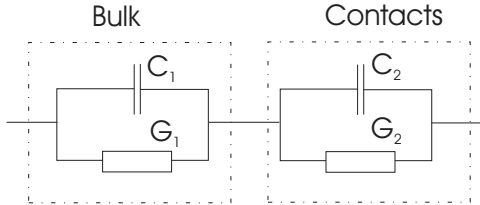


FIG. 4: Equivalent circuit for combination of bulk and surface components.

will be an important argument in considerations below.

As we can see from figures 2 and 3, our dielectric data can be represented quite well by Debye equivalent circuit consisting of capacitance in series with resistance²³. High frequency capacitance, when parasite capacitance is subtracted, gives $\varepsilon_{HF} \approx 30$, as expected for perovskites. Low frequency capacitance of sample P1 gives colossal values of $\varepsilon(0) \approx 5000$. In order to verify these data, we have measured four polycrystalline samples and four single crystals and, although varying considerably, dielectric constant always shows "colossal" values above 10^3 . Dielectric constant and relevant data for all 8 samples are presented in Table 1. Value of dielectric constant is de-

sample	area (mm ²)	thickness (mm)	contact type	R_{RT} (Ω)	$C(0)$ (nF)	$\varepsilon(0)$
P1	12	0.5	Agpaint	10	1	$5 \cdot 10^3$
P2	13.2	1.2	filmAu	9	2	$2 \cdot 10^4$
P3	7	1.2	filmAu	24	9	$1.7 \cdot 10^5$
P4	4.1	0.63	Agpaint	20	0.12	$3 \cdot 10^3$
S1	9	0.25	Agpaint	2	0.4	$1.3 \cdot 10^3$
S2	9	0.65	Agpaint	3	0.25	$2 \cdot 10^3$
S3	7.2	0.58	Agpaint	54	0.14	$1.3 \cdot 10^3$
S4	2.9	1.4	filmAu	35	5	$4.5 \cdot 10^4$

TABLE I: Some relevant parameters of eight samples in this study. All resistances are from two-contact measurements

duced by extrapolation of flat part of ε' (i.e. at $\omega \ll \omega_0$) toward zero frequency. One can see that lowest dielectric constant (and capacitance) have samples with contacts made directly with silver paint. Samples with preevaporated gold contacts show much higher dielectric constant: $\varepsilon(0) \geq 10^4$ despite higher (or just because of it!) contact resistances. This finding is even emphasized by large difference of $C(0)$ on the same sample (S3) for two different types of contacts. It can be also seen that capacitance doesn't depend (at least significantly) on geometrical factors. All of the above suggest that dielectric response in PCMO is governed by contacts.

In Figure 4 we present a typical equivalent circuit that represents both bulk and surface (blocking) capacitances. Both of them are parallely accompanied by their corresponding resistances or, as noted in the Figure 4, by conductances $G_i = 1/R_i$. Zero frequency capacitance $C(0)$ for

such a circuit is given by:

$$C(0) = \frac{G_1^2 C_2 + G_2^2 C_1}{(G_1 + G_2)^2} \quad (3)$$

In the high temperature limit we assume $G_2 \ll G_1$ that yields to $C(0) = C_2$ and in low temperature limit $G_2 \gg G_1$ yielding $C(0) = C_1$. Between these two limits we have complex interplay of conductances G_1 and G_2 that determinates capacitance $C(0)$ and relaxation time τ_0 . Let's now assume that bulk capacitance C_1 equals to high frequency limit of capacitance in Fig. 2, i.e. $C_1 = 10\text{pF}$. Surface or contact capacitance is then the one of low frequency limit, i.e. $C_2 = 1\text{nF}$. As we saw from Fig.1, contact resistance at low temperatures diminishes comparing to bulk resistance. Capacitance is in this, low temperature limit given by $C = (G_1^2/G_2^2)C_2 = (R_2^2/R_1^2)C_2$. In this way the diminishing contribution of contact resistance can explain the decrease of capacitance at low temperatures (as is evident from Fig 2). Relaxation time τ_0 in low temperature limit ($G_2 > G_1$) is given predominantly by G_1 , like in the typical Debye case ($R_1 = 1/G_1$ in series with C_2). This gives the same temperature dependence of τ_0 as shown in Fig.3. Note further that two definitions of τ_0 plotted in Fig.3 differ more at high temperatures and converge toward low temperatures. This convergence illustrates diminishing contribution of contact resistance R_2 in $R = R_1 + R_2$ since real relaxation time τ_0 (measured by dielectric relaxation) is defined by bulk resistance $\tau_0 = R_1 C_2$ and not by overall resistance $R = R_1 + R_2$. Our low-frequency relaxation thus seems to come from contact capacitances. Finally, to successfully fit our data to the combination of bulk and surface elements like in Fig.4, we assumed that element C_2 is not ideal but the universal capacitance. This means that C_2 is frequency dependent ($C_2 = B(i\omega)^{n-1}$) which actually simulates the distribution of different contact capacitances coming from irregularities at the contact interfaces. Such an assumption is necessary to successfully fit broadened relaxation ($n < 1$) from Fig. 2. Fit for $T = 80\text{K}$ is shown as a solid line in Fig.2.

In Table 1 we have listed values of capacitances $C(0)$ for our eight samples. These are the values at room temperature (RT) that are either measured directly or deduced from the low temperature measurements. Namely, due to small resistance of PCMO samples at room temperature, dielectric measurements are impeded by both inductances and sensitivity of measuring instrument, especially at low frequencies. Thus, we were able to record RT capacitances directly only in samples with high $C(0)$. Figure 5 presents $C(0)$ values for four of our samples up to (and above) room temperature. One can see once again that the capacitance increases with temperature and becomes nearly temperature independent toward RT. This justifies our estimate of RT capacitances of other four samples. However, Figure 5 reveals a weak anomaly at temperatures close to T_{CO} . The model from Fig. 4 can not explain the decrease of $C(0)$ at $T > T_{CO}$. It appears

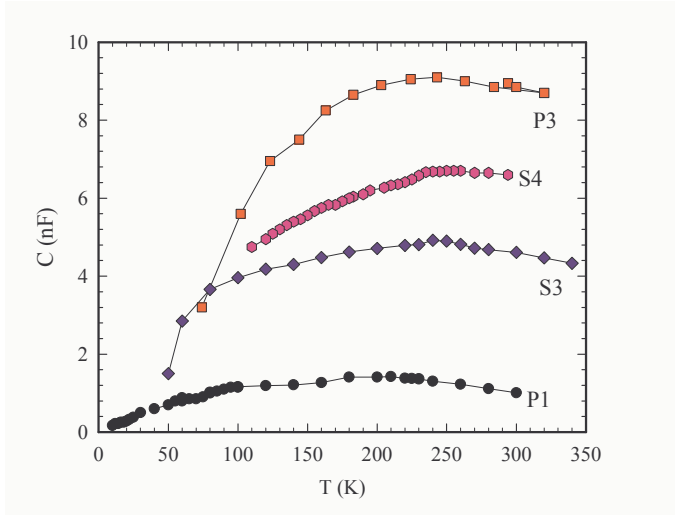


FIG. 5: (Color online) Temperature dependence of capacitance $C(0)$ for four different samples.

that dielectric response in PCMO is influenced by bulk properties, indeed. Let's probe it by other methods.

Measurements in magnetic field

The influence of magnetic field on dielectric response in PCMO is clearly one of the most intriguing questions, having in mind colossal effects of magnetic field on materials resistance. Figures 6a and 6b present the influence of magnetic field on the real part of capacitance C for $T=80\text{K}$ and $T=30\text{K}$, respectively, for single crystal sample S3. Insets present d.c. resistance curves in field. These insets are excellent examples of colossal magnetoresistance effect. At field strengths above several tesla, the resistance drops for several orders of magnitude. This is the consequence of magnetic field induced ferromagnetic transition²⁴. Our magnetization measurements, as well as hysteresis in resistive measurements, show that these transitions are of first order. At $T=80\text{K}$, the resistance decreases rather smoothly in magnetic field until first order transition field of $B_m=7.35\text{T}$ (as deduced by magnetization measurements) that is indicated by vertical line. At $B=0\text{T}$ resistance is already low enough and we observe relaxation in our frequency window. In this resistance range τ_0 is given mainly by $R_1=1/G_1$ and decrease of resistance enables us to follow adjacent decrease of relaxation time τ_0 . At the same time, capacitance remains roughly constant. From the data presented in Fig. 6a we see that this case resembles very closely the ordinary, zero-field temperature dependence (Fig. 2). Note also that the relaxation observed in 80K case is at fields lower than B_m .

Situation is different at $T=30\text{K}$. At 30K and zero magnetic field dielectric relaxation falls below our frequency window ($f_0 < 20\text{Hz}$). Therefore, what we see at this field is high frequency tail of our relaxation giving high-frequency dielectric function $\epsilon_{HF} \approx 30$. However, with increasing field, i.e. decreasing resistance,

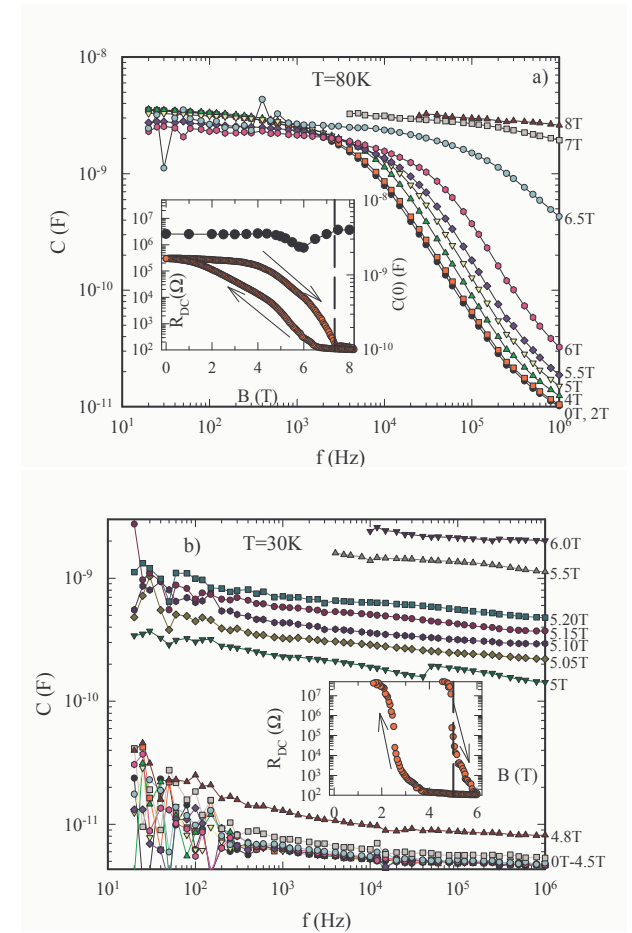


FIG. 6: (Color online) Effect of magnetic field on capacitance at a) $T=80\text{K}$ and b) $T=30\text{K}$ for sample S3. Values of magnetic field are given on the right axis. Insets show d.c. resistance as a function of field. Broken lines indicate ferromagnetic transition B_m as deduced from up-field magnetization measurements. Solid circles in inset of 6a denote capacitance $C(0)$.

one would expect to see low-frequency relaxation reappearing as in Fig. 2a. Instead, dielectric response increases abruptly, keeping its frequency independent (flat) shape to the highest fields. It is difficult to explain a raise of capacitance at constant temperature for different fields/resistances if one would assume single element (bulk) source. But if one assumes double capacitances like in Fig. 4, one can simulate this increase. Modeling resistances from eq. 3 approximately yield to $C(0) \propto R_2^2/R_1^2$. Raise of capacitance thus suggests that contact resistance R_2 doesn't decrease with field as fast as bulk resistance R_1 . This shouldn't be unexpected if one recalls that contact region should be the region with larger imperfections. Since the bulk insulator-metal transition is connected with ferromagnetic ordering, it is expectable that ferromagnetic ordering (i.e smaller resistance) is impeded at sample boundaries, close to electrodes. Such an interpretation is in accordance with

rather high resistance ($R=R_1+R_2=100\Omega$) above B_m - this resistance is presumably coming from contacts. In this way interplay of resistances $R_1=1/G_1$ and $R_2=1/G_2$ give the same increase of $C(0)$ like in Figure 2a. The interesting phenomena is that 30K case lacks the relaxation that would be expected from gradual decrease of R_1 (capacitance in Fig.6b is nearly flat in frequency). This experimental fact is confirmed in other samples and is always connected with ferromagnetic state at fields above B_m . It seems that relatively simple equivalent diagram in Fig.4 does not represent well our system in ferromagnetic phase. Lack of relaxation might indicate strong correlation effects in ferromagnetic phase. Dielectric response of systems with strong correlation is rigid, i.e. it does not relax²³. This is exhibited by flattening/disappearance of the loss peak and corresponding effect in its real counterpart. Contrary to this, at $T=80K$ we observe the relaxation since these measurements are done in anti-ferromagnetic phase ($B < B_m$), equally as measurements without magnetic field. Bulk and contact resistance here depend similarly on magnetic field (see figure 1) and $C(0)\propto R_2^2/R_1^2$ remains approximately constant. Small twist of $C(0)$ around $B=6T$ can be associated exactly to the change in resistance ratio R_2/R_1 close to ferromagnetic transition.

Measurements with d.c. bias

As already mentioned in introduction, the PCMO system is susceptible to applied electric field, the effect that for high voltages leads to insulator-metal transition. But even below this threshold field, the current-voltage characteristic is nonlinear showing decrease of resistance with increase of voltage. This nonlinearity can not be explained solely by heating effects since at temperatures below 60K it is observed even for heating power less than 1pW. It is therefore interesting to see the effect of voltage on dielectric response. We have performed dielectric measurements for a set of a.c. excitation voltages and also those biased by d.c. voltage. They are essentially identical so we present here just d.c. biased measurements. Figure 7 shows such measurements for single crystal S3 at $T=80K$. Capacitance is shown for a set of d.c. bias voltages ($V_{bias}=0, 20, 40, 80, 160, 320, 640$ and 1280mV). The a.c. excitation was always kept at the lowest level of $V=20mV$. In the upper right inset is the effect of bias on sample resistance (circles - left axis) and relaxation time τ_0 (diamonds - right axis). Resistance decreases for more than one order of magnitude for this range of voltages. Its origin is clearly not heating since resistance at this temperature decreases even for heating power of 10nW. As in all previous (zero-bias) cases in this study, the relaxation time τ_0 follows the resistance, i.e. decreasing resistance is accompanied by decreasing τ_0 . However, we can see that this correspondence is not perfect: τ_0 decreases nine times while resistance drops twenty-two times. If we recall our model in Fig.4, and remember that $\tau_0\propto R_1$, this means that contact resistance R_2 coming from our measured resistance R ($R=R_1+R_2$) is responsible for stronger decrease of R than expected

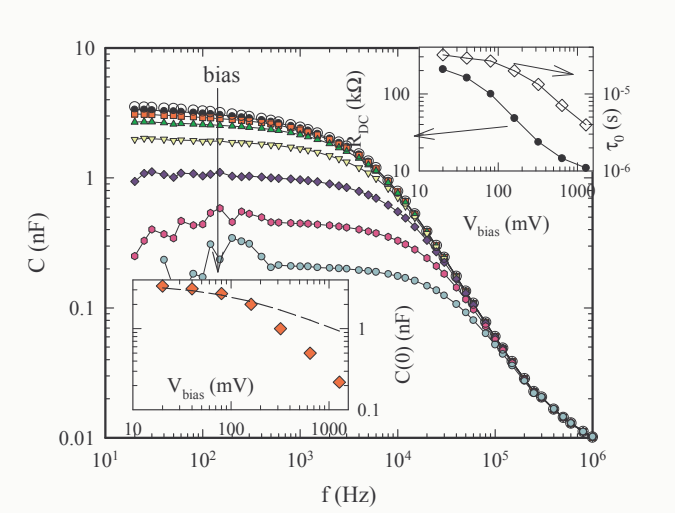


FIG. 7: (Color online) Effect of d.c. bias on capacitance at $T=80K$ for sample S3. Arrow indicates increasing bias voltage - voltages are as shown in the inset. Right inset: resistance R_{DC} (circles, left axis) and relaxation time τ_0 (diamonds, right axis) as a function of d.c. bias voltage. Left inset: capacitance $C(0)$ (diamonds) vs. bias voltage. Broken line is an estimate according to eq. 4.

from $\tau_0\propto R_1$. But the most important feature here is the decrease of capacitance with bias voltage (and decreasing resistance). This effect is opposite than observed at temperature dependence of non-biased measurements (see for example Fig. 3).

It is well known that metal-semiconductor contact usually results in Schottky barrier. A region of semiconductor in direct contact with metal is depleted of carriers as a consequence of different band levels in both materials. This depletion layer thus depends on type of metal, i.e. its energy band. The width w of depletion layer is given by

$$w = \sqrt{\frac{2\varepsilon}{qN_D}(V_b - V_a)} \quad (4)$$

where V_b stands for internal, junction voltage and V_a for external, applied voltage. ε is dielectric constant of semiconductor, q electron charge and N_D impurity concentration. Schottky contacts always present a capacitance $C=\varepsilon S/w$ that, as seen from eq. 4, depends as $C\propto w^{-1}\propto(V_b-V_a)^{-1/2}$. In ideal Schottky semiconductor case (one contact perfectly ohmic and another with Schottky barrier) applied voltage V_a is supposed to be in reverse direction (negative) in order to decrease capacitance. In our case that has two equivalent Schottky contacts, situation becomes more complicated. But overall behavior is the same. In the left inset we plot $C(0)$ vs. V_{bias} as deducted from Fig.7. We also plot a line that fits to calculated data and is calculated by eq. 4 using $V_b=0.1V$, as estimated roughly from $R(T)$ measurement. This estimate fits quite well to measured data

for small voltages, i.e. for voltages smaller than Schottky breakthrough voltage. The decrease of capacitance with voltage can be therefore interpreted by Schottky effect. And finally, current-voltage nonlinearity (shown in our case as decreasing resistance with applied voltage) is the basic property of Schottky diodes. It thus becomes evident that dielectric response in PCMO, as well as related nonlinear effects, has the origin in Schottky barriers at metallic contacts. This also explains dependence of capacitances on type of contacts (Au film or Ag paint).

Summary

We have performed detailed analysis of "colossal" dielectric response in $\text{Pr}_{0.6}\text{Ca}_{0.4}\text{MnO}_3$. Dielectric relaxation and decrease of capacitance at low temperatures are associated with the interplay of surface and bulk capacitances and their related resistances. Change of capacitance with magnetic field can be equally well explained by surface (contact) capacitances. Dependence of dielectric response on voltage (both d.c. and a.c.) can be explained only as a consequence of Schottky layers in contact with electrodes. This interpretation is in accordance with dependence of capacitance on metal used as the electrode. All of the above suggest that bulk properties of title material are not responsible for dielectric response: dielectric constant of title material is $\varepsilon(0)=\varepsilon_{HF}=30$, of the same order of magnitude as in other perovskites²⁶. None of the intriguing physical properties of PCMO (charge ordering, antiferro and ferromagnetism, clusters) seem to influence dielectric response. The only feature resembling to bulk property of PCMO is a weak anomaly at temperatures close to temperature of charge ordering. Decrease of capacitance with temperature for $T > T_{CO}$ can not be explained in the frame of diagram in Fig. 4. However, it might be evident that contact (Schottky) capacitance C_2 can be temperature dependent through internal voltage V_b . This can lead to slight increase of C_2 with lowering temperature. And at low temperatures we enter into regime described by Fig. 4. As can be seen from 4-contacts resistance curve of sample S3 in Fig. 1, bulk re-

sistance of PCMO increases rapidly at T_{CO} . This rapidly influences the balance of resistances in Fig. 4, resulting in decrease of overall capacitance. Thus, T_{CO} anomaly can be again interpreted as interplay of bulk and contact capacitance.

The temperature dependence of dielectric constant in Ref.²¹ generally agrees with those presented here. The most visible difference is much stronger anomaly at $T=T_{CO}$ in Ref.²¹. We interpret this by different contact material (GaIn paint) that was used in that study. Since contacts depend on type of metal used, it should be expected that contact capacitances have different temperature dependence and also different breakdown voltages. Usage of rather high voltage of $V=1\text{V}$ in this study could additionally influence Schottky capacitances.

Our measurements, in accordance with some reports²⁵, suggest strongly that all reports of apparently colossal dielectric constant should pass detailed analysis in order to eliminate the possibility of Schottky barrier capacitances as the origin of anomalously large dielectric constant. As for the family of PCMO manganites, we hope that we proved such an origin. Our finding is emphasized by apparently colossal dielectric constant in other manganites ($\text{CuCa}_3\text{Mn}_2\text{Ti}_2\text{O}_{12}$) that, contrary to PCMO, lack charge ordering or structural inhomogeneities²⁷.

Finally, it is worth to give one more comment about the colossal effect of magnetic field on dielectric response in title material (Fig. 6). This "magnetocapacitive" or "magnetodielectric" effect, has recently attracted considerable interest^{28,29,30}. We have demonstrated here that colossal magnetocapacitive effects can also arise from purely non-intrinsic contributions.

Acknowledgments

We acknowledge financial support from Ministerio de Educación y Ciencia (MAT2003-01880) and Comunidad de Madrid (07N/0080/2002). We are very grateful to R. Jiménez Riobóo, for enlightning discussions.

* Electronic address: biskup@icmm.csic.es

¹ M.A. Subramanian, D. Li, N. Duan, B.A. Reisner and A.W. Sleight, J. Solid State Chem. **151**, 323 (2000).

² M.H. Cohen, J.B. Neaton, L.X. He, D. Vanderbilt, Jour. Appl. Phys. **94**, 3299 (2003); L.X. He, J.B. Neaton, M.H. Cohen, D. Vanderbilt, C.C. Homes, Phys. Rev. B **65**, 214112 (2002).

³ P.Lunkenheimer, R.Fichtl, S.G.Ebbinghaus and A.Loidl, Phys. Rev. B **70**, 172102 (2004).

⁴ For the review of this subject see E.Dagotto, T.Hotta and A.Moreo, Physics Report **344**, 1 (2001) or M.Ziese, Rep. Prog. Phys. **65**, 143 (2002).

⁵ M.Uehara, S.Mori, C.H.Chen, S.-W.Cheong, Nature **399**, 560 (1999).

⁶ M.Fäth, S.Freisem, A.A.Menovsky, Y.Yamioka, J.Aarts and J.A.Mydosh, Science **285**, 1540 (1999).

⁷ Y.Tomioka, A.Asamitsu, H.Kuwahara, Y.Moritomo and Y.Tokura, Phys. Rev. B **53**, R1689 (1996).

⁸ Z.Jirak, S.Krupicka, Z.Simsa, M.Dlouha, Z.Vratislav, J. Magn. Magn. Mater. **53**, 153 (1985).

⁹ H.Yoshizawa, H.Kawano, Y.Tomioka and Y.Tokura, Phys. Rev. B **52**, R13145 (1995).

¹⁰ A.Asamitsu, Y.Tomioka, H.Kuwahara and Y.Tokura, Nature **388**, 50 (1997).

¹¹ Y.Moritomo, H.Kuwahara, Y.Tomioka, Y.Tokura, Phys. Rev. B **55**, 7549 (1997).

¹² V.Kiryukhin, D.Casa, J.P.Hill, B.Keimer, A.Vigilante, Y.Tomioka and Y.Tokura, Nature **386**, 813 (1997).

¹³ J. Sichelschmidt, M. Paraskevo, T. Brando, R. Wehn, D. Ivannikov, F. Mayr, K. Pucher, J. Hemberger, A. Pimenov, H.A.K. von Nidda, P. Lunkenheimer, V.Y. Ivanov, A.A. Mukhin, A.M. Balbashov, A. Loidl, Eur. Phys. J. B

²⁰, 7 (2001).

¹⁴ A.Anane, J.P.Renard, L.Reversat, C.Dupas, P.Veillet, M.Viret, L.Pinsard and A.Revcolevschi, Phys. Rev. B **59**, 77 (1999).

¹⁵ S. Katano, J.A. Fernandez-Baca, Y. Yamada, Physica B **276-278**, 786 (2000).

¹⁶ P.G. Radaelli, R.M. Ibberson, D.N. Argyriou, H. Casalta, K.H. Andersen, S.W. Cheong and J.F. Mitchell, Phys. Rev. B **63**, 172419 (2001).

¹⁷ R.Kajimoto, T.Kakeshita, Y.Oohara, H.Yoshizawa, Y.Tomioka, Y.Tokura, Phys. Rev. B **58**, R11837 (1998).

¹⁸ J.Tao and J.M.Zuo, Phys. Rev. B **69**, 180404(R) (2004).

¹⁹ E.Dagotto, cond-mat/0302550v1 (2003).

²⁰ F. Rivadulla, M.A. López-Quintela, L.E. Hueso, C. Jardón, A. Fondado, J. Rivas, M.T. Causa and R.D. Sánchez, Solid State Commun. **110**, 179 (1999); C. Jardón, F. Rivadulla, L.E. Hueso, A. Fondado, M.A. López-Quintela, J. Rivas, R. Zysler, M.T. Causa, R.D. Sánchez, J. Magn. Magn. Mater. **196**, 475 (1999);

²¹ S.Mercone, A.Wahl, A.Pautrat, M.Pollet, C.Simon: Phys. Rev. B **69**, 174433 (2004).

²² "Electronic Processes in Non-crystalline Materials", Mott and Davis, Clarendon Press, Oxford (1971).

²³ "Dielectric Relaxations in Solids", A.K.Jonscher, Chelsea Dielectric Press, London (1983).

²⁴ Y.Tomioka, A.Asanitsu, Y.Moritomo and A.Tokura, J. Phys. Soc. Jpn **63**, 1689 (1995).

²⁵ P. Lunkenheimer, V. Bobnar, A.V. Pronin, A.I. Ritus, A.A. Volkov, A. Loidl, Phys. Rev. B **66**, 052105 (2002).

²⁶ L. He, J.B. Neaton, M.H. Cohen and D. Vanderbilt, Phys. Rev. B **65**, 214112 (2002.); D. Capsoni, M. Bini, V. Massarotti, G. Chiodelli, M.C. Mozzatic, C.B.Azzoni, J. Solid. State. Chem. **177**, 4494 (2004).

²⁷ N.Biškup, to be published.

²⁸ T. Kimura, T. Goto, H. Shintani, K. Ishizaka, T. Arima, Y. Tokura, Nature **426**, 55 (2003).

²⁹ J. Hemberger, P. Lunkenheimer, R. Fichtl, H.-A. Krug von Nidda, V. Tsurken, A. Loidl, Nature **434**, 426 (2005).

³⁰ N. Hur, S. Park, P.A. Sharma, S. Guha, S.-W. Cheong, Phys. Rev. Lett. **93**, 107207 (2004).